Placenta 88 (2019) 28–35

Contents lists available at ScienceDirect

Placenta

journal homepage: www.elsevier.com/locate/placenta

The effect of maternal hyperoxygenation on placental perfusion in normal and Fetal Growth Restricted pregnancies using Intravoxel Incoherent Motion

Ting Chen[a], Meng Zhao[a,*], Jiacheng Song[a,**], Xihu Mu[a], Yong Jiang[a], Xin Zhou[b], Xuanyi Zhou[c], Yongming Dai[c]

[a] Department of Radiology, The First Affiliated Hospital of Nanjing Medical University, Nanjing, 210029, China
[b] Department of Obstetrics & Gynecology, The First Affiliated Hospital of Nanjing Medical University, Nanjing, 210029, China
[c] United Imaging Healthcare, MR Collaboration, Shanghai, 201302, China

ARTICLE INFO

Keywords:
Placenta
Perfusion
IVIM
FGR
Maternal hyperoxygenation

ABSTRACT

Purpose: To evaluate the effect of maternal hyperoxygenation on placental perfusion in normal and Fetal Growth Restricted (FGR) pregnancies using Intravoxel Incoherent Motion (IVIM).

Methods: Ten FGR pregnancies and twenty-five normal pregnancies underwent IVIM examinations before and after maternal hyperoxygenation (95% O_2, 5% CO_2) using a 1.5T MR scanner. The IVIM parameters (f_p, D_t, D_p) were determined for the placentas of both groups. The IVIM parameters within and between groups and their correlations with Doppler findings were statistically analyzed. ROC analysis was performed to evaluate the diagnostic power of IVIM derived parameters.

Results: Before maternal hyperoxygenation, the perfusion fraction f_p was significantly lower in the FGR group than that in the normal group ((%) vs. 36.28 ± 9.70 (%), $p = 0.000$). After maternal hyperoxygenation, f_p decreased significantly in the normal group (36.28 ± 9.70 (%) vs. 29.93 ± 10.25 (%), $p = 0.032$), whereas it remained relatively stable in the FGR group ((%) vs. 24.38 ± 13.67 (%), $p = 0.508$). An increase of D_t was found only for the normal group and D_p did not changed significantly after maternal hyperoxygenation. There existed a negative correlation between $f_{p\ pre}$ and umbilical artery pulsatility index (PI) ($r = -0.385$, $p < 0.05$) as well as $D_{t\ post}$ and PI ($r = -0.574$, $p < 0.01$). The $f_{p\ pre}$ displayed a best diagnostic power of all parameters with the area under curve (AUC) of 0.912.

Conclusion: The perfusion fraction, f_p, is able to distinguish FGR from normal pregnancies by its value pre and by its change (or lack thereof) post maternal hyperoxygenation. IVIM may potentially help improve the diagnosis of placenta function as it relates to disease.

1. Introduction

As one common disease suffered by innumerable prenatal fetus, Fetal growth restriction (FGR) is clinically diagnosed with the classical standard: fetus weight not able to achieve the expected growth potential—below the threshold of 10th centile as well as some newer diagnostic markers including maternal angiogenic factors, Doppler cerebroplacental ratio, uterine artery Doppler and so on were introducing for the better diagnosis of FGR [1]. Notoriously causing poor pregnancy outcome including neonatal morbidity, high neonatal mortality, high rate of stillbirths, FGR is urgently needing timely and effective prenatal treatment [2,3].

The most distinguishable abnormalities of FGR include the increased vascular resistance as well as the peripheral hypovascularity [4–6], leading to the far more limited microcirculation with regard to the normal counterparts. As well-known during clinical practice, the weakened microcirculation will definitely result in the severe impeditive circulation of nutrient and oxygen, which, as a result, leads to the uteroplacental hypoxia and other related syndromes. Therefore, during the past few decades, a great deal of efforts have been made to explore the therapeutic strategies for improving the weakened placental circulation of nutrients and oxygen [7–9]. Due to the capability of improving the placental oxygen level directly and obviously [10], the effect of maternal oxygenation was investigated for improving placental perfusion by a lot of researchers [10,11]. However, the real effect of maternal hyperoxygenation and its therapeutic value still remains

* Corresponding author. Department of Radiology, The First Affiliated Hospital of Nanjing Medical University, No. 300, Guangzhou Road, Nanjing, 210029, China.
** Corresponding author.
E-mail addresses: zhaomengnanjing@sina.com (M. Zhao), yysjc1990@163.com (J. Song).

https://doi.org/10.1016/j.placenta.2019.08.078
Received 21 March 2019; Received in revised form 5 July 2019; Accepted 7 August 2019
Available online 07 August 2019
0143-4004/

unclear, which greatly limited the further clinical application of oxygen therapy. Except the complex unknown biological basis, one important reason lies in that Color Doppler, widely applied in current clinical practice for evaluating placental circulation, owns a lot of insurmountable disadvantages including low sensitivity, experience-dependent diagnose, poor repeatability and so on. Undoubtedly, cutting-edge and powerful techniques are urgently needed.

Not only inheriting many superiorities from Magnetic Resonance Imaging (MRI) such as high soft-tissue resolution, non-ionization radiation, arbitrary image orientation imaging and so on, but DWI can provide a lot of biological implication concerning the cellularity, vascularity and micro-structure [12]. As one advanced bi-exponential DWI model, Intravoxel incoherent motions (IVIM) holds great potential in evaluating perfusion variation especially with the assistance of functional parameters including f (perfusion fraction) representing the capillary fraction as well as D^* representing the vessel flow velocity [13]. For instance, Siauve proposed that f is effective in quantifying the perfusion change as the function of gestational age [14].

Therefore, this research, to the best of our knowledge, for the first time aims to unveil the effects of maternal hyperoxygenation on placental perfusion in both FGR patients and Normal counterparts. Besides, the diagnostic value of IVIM derived parameters for discriminating the FGR patients from normal counterparts was also evaluated through statistical analysis.

2. Materials and methods

2.1. Subjects

This research, carried out from April, 2017 to October, 2018, was approved by the Nanjing Medical University Ethics Committee. (Ethics approval number: 2017-SRFA-087). The informed written consent from each participant was successfully obtained.

2.1.1. Inclusion criteria

Obstetrics and Gynecology textbook (7th edition) [15] was applied as the diagnostic standard of FGR patients: Fetal weight (> 37 weeks) was below 2500 g or it is less than the 10% percentile of the expected growth potential calculated via standard curve; Or it is less than twice the standard deviations of the fetus average weight with same gestational week.

2.1.2. Exclusion criteria

1) MR images with poor quality due to severe artifacts.
2) Inaccessible IVIM results.
3) Some maternal diseases including hypertension, pre-existing renal disease and diabetes mellitus closely associated with the unexpected influence on perfusion.
4) Rejection of magnetic resonance scan due to many reasons including claustrophobia, safety concern and so on.
5) Placental abnormalities containing placenta previa, abnormal placental implantation, vasa previa and placental abruption.

Thirty-one apparently normal singleton pregnancies with gestational age of 22–34 weeks without abnormal placental ultrasound findings such as placenta previa, abnormal placental implantation, vasa previa and placental abruption were enrolled into normal patients group. Twelve pregnancies, diagnosed as FGR according to the standard noted in the aforementioned inclusion criteria, were included into FGR patients group. Two patients with poor MR image quality due to severe artifact were excluded in FGR patients group. Five patients in normal group were excluded because IVIM based MR scan was not performed. One patient with poor image quality together with two patients with hypertension were also excluded. Finally, there were ten and twenty-five patients enrolled into the group of FGR patients and normal patients, respectively.

2.2. MR imaging

All pregnancies were examined with a conventional 1.5 T MR scanner (uMR560, United Imaging Healthcare; Shanghai, China) with a combination of a twelve-channel surface body coil and two embedded spine coils. All women were imaged either in the supine (41 pregnancies) or lateral position (2 pregnancies) for comfort purposes.

MR protocols included a T1-weighted gradient echo sequence in sagittal direction (repetition time (TR)/echo time (TE) = 8.4/3.2 msec; flip angle (FA) = 70°; slice thickness = 4.0 mm), T2-weighted turbo spin echo sequence in coronal, transversal and sagittal directions (TR/TE = 1400/92 msec; slice thickness = 4.0 mm, turbo factor = 2), and T2-weighted balanced steady state free procession sequence (TR/TE = 5/2.5 msec; FA = 70°; slice thickness = 3.0 mm). The field of view (FOV) varied from 350 to 400 mm^2 and the matrix size varied from 256 to 448 to keep the in-plane resolution roughly 1.5 × 1.5 mm^2.

IVIM was performed before and immediately after maternal hyperoxygentation based on a single-shot echo-planar imaging (EPI) sequence (TR/TE = 4000/73.6 msec; echo spacing, 0.58 msec; slice thickness, 4 mm; in-plane resolution 3.5 × 3.5 mm^2; total acquisition time, 5.5 min) with a spectrum of different b-values of 0, 20, 40, 80, 160, 200, and 500 s/mm^2. With T2-weighted images as a reference, the orientation of the IVIM imaging slices was placed to make the lateral side placenta in the center of the image.

The maternal hyperoxygenation was completed in between the first and second IVIM examinations. After the first IVIM examination, pregnancies were provided a non-rebreather facial mask (Hudson Respiratory Care, Durham, NC) for an episode of ten-minute oxygenation inhalation (12L, 95% O_2 and 5% CO_2 per minute) inside the MR bore to minimize movement during examinations.

2.3. Image analysis

IVIM post-processing based on the multi b-value diffusion weighted images were performed using Osirix software (Osirix, https://www.osirix-viewer.com/osirix/osirix-md/) with the following bi-exponential model.

$$S(b) = S_0 \cdot [(1 - f_p) \cdot \exp(-b \cdot D_t) + f_p \cdot \exp(-b \cdot D_p)] \quad (1)$$

where $S(b)$ is the signal intensity at a given b-value and S_0 is the signal intensity at b-value = 0 s/mm^2. f_p stands for the volume fraction of the vascular compartment with its corresponding diffusion coefficient, D_p (pseudodiffusivity). $(1 - f_p)$ stands for the remaining volume fraction, tissue or cellular compartment, with its corresponding diffusion coefficient, D_t (true diffusivity). Parametric maps for f_p, D_t and D_p were generated by voxel-wise fits to equation (1) using all b-values. Fig. 1 showed an example of bi-exponential fitting results of an ROI drawn on IVIM images of one normal placenta.

Two radiologists in fetal MRI (5 and 7 years' experience, respectively) who were blinded to patients' information analyzed IVIM results independently in an in-house developed software SPIN (Signal Process in Nmri, SpinTech, Bingham Farms, MI, USA). Poor image quality due to fetal or maternal motion were excluded. For each subject, a reference slice of EPI at a b-value = 0 s/mm^2 that contained the largest volume of placenta was determined in consensus, then the corresponding slices in all parametric maps were chosen as representative ones for further analysis. A region of interest (ROI), no less than 50 mm^2, was drawn in the center of placenta (between decidual and chorionic plates) on the reference slice by two radiologists, respectively. The ROIs defined on the reference slice were automatically generated on the representative parametric slices in software as they were spatially matched, Fig. 2. The mean values of ROIs were recorded for further analysis.

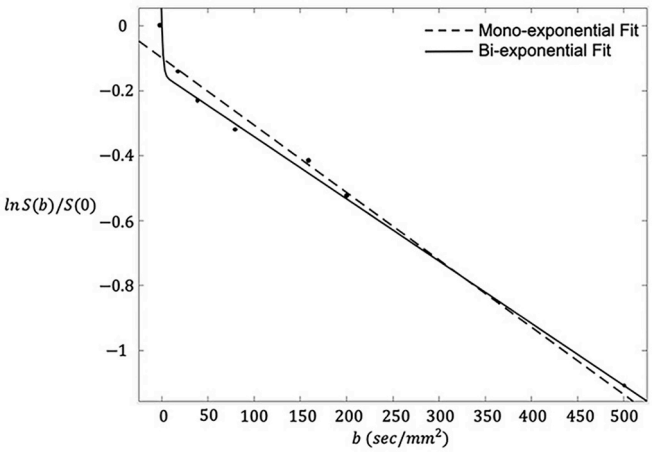

Fig. 1. Graphs plot signal attenuation - $\ln\left(\frac{s(b)}{s(0)}\right)$ based on the mean value of an arbitrary ROI drawn in placenta, where $s(b)$ is the signal intensity at a specific b-value, $s(0)$ is the signal intensity at b-value = 0 mm^2/s. The solid and dotted lines were the fitting results based on bi-exponential and mono-exponential models, respectively.

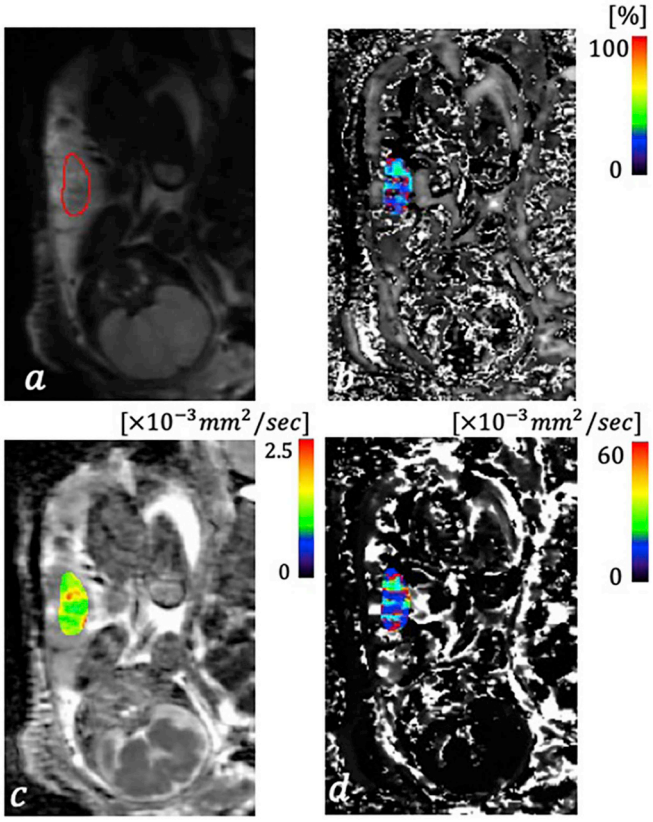

Fig. 2. An example of IVIM result obtained before maternal hyperoxygenation from a normal pregnancy (26 years, 28 gestational weeks). a) Diffusion weighted image at b-value = 0 mm^2/s; b) Perfusion fraction, f_p, map; c) True diffusivity, D_t, map; d) Pseudodiffusivity, D_p, map. The ROI was drawn on diffusion weighted image (b = 0 mm^2/s) and then transferred to the other three maps with corresponding pseudo color bar indicating the range of value.

2.4. Statistical analysis

Inter-observer reliability for the categorical items was analyzed by Cohen's kappa method. A prior classification of chuκ value were as follows: $\kappa = 0$, no agreement; $0 < \kappa \leq 0.2$, slight agreement, $0.2 < \kappa \leq 0.4$, fair agreement; $0.4 < \kappa \leq 0.6$, moderate agreement; $0.6 < \kappa \leq 0.8$, substantial agreement and $\kappa > 0.8$, near perfect agreement. All IVIM parameters belonging to different groups or obtained before and after maternal hyperoxygenation were denoted by the subscript "normal", "FGR", "pre" and "post". Additionally, the relative percentage change of perfusion fraction, defined as $\Delta f = \frac{f_{p,post} - f_{p,pre}}{f_{p,pre}} \times 100\%$, was analyzed. The Shapiro-Wilk W test was performed to evaluate whether each IVIM-derived parameter followed the normal distribution. The Wilcoxon rank sum test was performed to compare the IMIM-derived parameters between FGR patients group and Normal patients group as well as those obtained pre and post the maternal hyperoxygenation. The Spearman correlative analysis was performed to determine the correlation between Doppler findings and IVIM-Derived parameters by the correlative coefficients abbreviated as r. Receiver operating characteristic (ROC) analysis was performed to evaluate the predictive value of IVIM-derived parameters for discriminating between normal patients and FGR patients. Diagnostic value of different IVIM-derived parameter was quantified and compared by the area under the ROC curve (AUC). All the statistical analyses were performed with MedCalc statistical Software version 15.6.1 (MedCalc Software bvba, Ostend, Belgium; http://www.medcalc.org; 2015). The statistical conclusions with significance were drawn by the p values of less than 0.05.

3. Results

3.1. Subjects characteristics

In total, 25 normal pregnancies (28 ± 3 years, gestational period 29 ± 2 weeks) and 10 FGR pregnancies (32 ± 6 years, gestational period 30 ± 1 weeks) were enrolled into this research. Table 1 summarized the clinical data of all FGR cases including the maternal characteristics, results from Doppler Ultrasonography examinations and their outcomes.

3.2. Inter-observer reliability

According to Cohen's kappa method, the agreement between two radiologists were 0.79 for D, 0.81 for f_p, 0.77 for D_p and 0.83 for D_t. Since all of them were in substantial or moderate agreement, then the average results were used in analysis.

3.3. Statistical comparison of IVIM derived parameter in the group of FGR patients and normal patients

As exhibited in Table 2, nearly all IVIM-derived parameters in FGR group and normal patients group did not follow the normal distribution according to the result of Shapiro-wilk W test. Thus, Wilcoxon rank sum test and Spearman correlation was performed for further statistical analysis.

Representative IVIM parametric map including f_p, D_t and D_p were displayed in Fig. 2. Moreover, as Fig. 3, Table 3 and Table 4 displayed, before maternal hyperoxygenation, the IVIM parameter $f_{p,pre}$ was significantly lower in the FGR group than that in normal group (22.88 ± 10.29 (%) versus 36.28 ± 9.70 (%), $p = 0.000$). Besides, significant difference was also found for the $D_{t,pre}$ ($1.22 \pm 0.29(10^{-3})mm^2/sec$ versus $1.47 \pm 0.23(10^{-3})mm^2/sec$, $p = 0.037$) but no significant difference for $D_{p,pre}$ ($51.82 \pm 53.28(10^{-3})mm^2/sec$ versus $63.42 \pm 54.18(10^{-3})mm^2/sec$, $p = 0.307$) was obtained.

After maternal hyperoxygenation, $f_{p,post}$ in the FGR group was still lower than that in normal group (24.38 ± 13.67 (%) vs. 29.93 ± 10.25 (%), $p = 0.058$). In addition, there existed significant difference for D_t (1.18 ± 0.19 $(10^{-3})mm^2/sec$ vs. 1.86 ± 0.42 $(10^{-3})mm^2/sec$, $p = 0.000$) with regard to no statistical difference for D_p ($83.05 \pm 63.84(10^{-3})mm^2/sec$ versus $63.08 \pm 35.38(10^{-3})mm^2/sec$,

Table 1
Information of FGR cases.

FGR	GA at MRI (week + day)	EFW (g)	Doppler findings	Outcome	Birth weight (g)	Δf (%)	Placental examinations
Case 1	31	1107	MCA: PI = 1.46 RI = 0.73 S/D = 3.38 UA: absence of end diastolic flow Placental thickness:5.3 cm	Elected CS Apgar score = 7-8 GA = 37 + 3	1200	−15.93	Accelerated maturation Distal villous hypoplasia Few infarcts and microcalcification Chronic inflammatory cell infiltration
Case 2	30 + 2	705	MCA: PI = 1.28 RI = 0.74 S/D = 3.89 MCA/UA ratio reversion Placental thickness:6.2 cm	Acute CS Apgar score = 8 GA = 33 + 1	997	24.80	Distal villous hypoplasia Few infarcts and degeneration few inflammatory cell infiltration
Case 3	30 + 6	1006	MCA: PI = 1.39 RI = 0.72 S/D = 3.62 UA: absence of end diastolic flow Placental thickness:3.2 cm	Acute CS Apgar score = 9 GA = 31 + 1	1060	10.73	Distal villous hypoplasia Increased intervillous fibrin Deposition and multiple calcification Focal infarcts Acute and Chronic inflammatory cell infiltration
Case 4	29 + 4	991	MCA: PI = 1.07 RI = 0.63 S/D = 2.73 UA: PI = 1.31 RI = 0.74 S/D = 3.90 Placental thickness:3.8 cm	Elected CS Apgar score = 8-9 GA = 30 + 4	1050	37.07	Distal villous hypoplasia Few infarcts Chronic inflammatory cell infiltration
Case 5	28	1075	MCA: PI = 1.49 RI = 0.725 S/D = 3.55 UA: S/D = 2.0 Placental thickness:3.4 cm	Elected CS Apgar score = 9-10 GA = 34 + 4	1580	−21.35	Placenta previa, placental accrete, placenta hemorrhage Multiple focal infarcts Marginal cord insertion
Case 6	33 + 3	1186	MCA: PI = 0.95 RI = 0.66 S/D = 2.93 UA: PI = 1.40 RI = 0.77 S/D = 4.42 absence of end diastolic flow Placental thickness:6.5 cm	Elected CS Apgar score = 9-10 GA = 33 + 5	1900	65.83	Maturation distal villous Few infarcts and calcifications Chronic inflammatory cell infiltration Central 3*4 cm^2 infarction area
Case 7	27	1732	MCA: PI = 1.41 RI = 0.74 S/D = 3.86 UA: PI = 1.15 RI = 0.67 S/D = 3.01 Placental thickness:2.9 cm	Elected CS Apgar score = 8 GA = 32 + 1	1850	19.96	Maturation distal villous Acute and Chronic inflammatory cell infiltration Few infarcts
Case 8	29		MCA: PI = 1.39 RI = 0.84 S/D = 3.06 UA: S/D = 5.72 Placental thickness:4.6 cm	Elected CS Apgar score = 9 GA = 32 + 1	1880	−28.01	Abnormal shape (velamentous placenta) Accelerated maturation of distal villous Increased intervillous fibrin and calcification deposition
Case 9	29 + 2	1392	MCA: PI = 2.24 RI = 0.87 S/D = 7.84 UA: PI = 0.96 RI = 0.60 S/D = 2.51 Placental thickness:5.4 cm	Elected CS Apgar score = 10 GA = 40	2250	20.66	Placenta accretes Maturation distal villous Few Chronic inflammatory cell infiltration normal shape
Case10	33 + 5	1137	MCA: PI = 1.26 RI = 0.71 S/D = 3.39	Elected CS Apgar score = 8 GA = 36 + 3	1550	−34.27	Maturation distal villous Multiple focal infarcts Amniotic membrane cyst 3.5*3*1 cm thrombotic vasculopathy of UA

(*continued on next page*)

Table 1 (*continued*)

FGR	GA at MRI (week + day)	EFW (g)	Doppler findings	Outcome	Birth weight (g)	Δf (%)	Placental examinations
			UA: PI = 1.60 RI = 1.87 S/D = 4.62 Placental thickness:3.9 cm				

Note.-* GA – gestational age, and all GA data in this table have a unit of week + day; EFW – estimated fetal weight; MCA – middle cerebral artery; UA – uterine artery; PI – pulsatility index; RI – resistance index; S – peak systolic velocity; D – end diastolic velocity of blood flow; CS – cesarean section; Δf is the relative percentage change of perfusion fraction, and $\Delta f = \frac{f_{p,post} - f_{p,pre}}{f_{p,pre}} \times 100\%$.

Table 2
The statistical results of Shapiro-Wilk W test for evaluating whether each IVIM-derived parameter followed the normal distribution.

Parameter	*p*	Normal Distribution	Parameter	*p*	Normal Distribution
$f_{p,pre,normal}$	0.020	NO	$f_{p,pre,FGR}$	0.003	NO
$f_{p,post,normal}$	0.912	Yes	$f_{p,post,FGR}$	0.008	NO
$D_{t,pre,normal}$	0.027	NO	$D_{t,pre,FGR}$	0.036	NO
$D_{t,post,normal}$	0.066	Yes	$D_{t,post,FGR}$	0.416	YES
$D_{p,pre,normal}$	0.001	NO	$D_{p,pre,FGR}$	0.004	NO
$D_{p,post,normal}$	0.021	NO	$D_{p,post,FGR}$	0.206	YES

Table 3
All IVIM parameters (mean ± standard deviation) for normal and FGR groups obtained before and after maternal hyperoxygenation.

	Normal		FGR	
	Pre	Post	Pre	Post
$f_p(\%)$	36.28 ± 9.70	29.93 ± 10.25	22.88 ± 10.29	24.38 ± 13.67
$D_t(10^3 mm^2/s)$	1.47 ± 0.23	1.86 ± 0.42	1.22 ± 0.29	1.17 ± 0.19
$D_p(10^3 mm^2/s)$	63.42 ± 54.18	63.08 ± 35.89	51.82 ± 53.28	83.04 ± 63.83

Note.-* FGR – Fetal growth restricted; Pre – before maternal hyperoxygenation; Post – after maternal hyperoxygenation.

$p = 0.559$) between FGR patients and normal patients.

Besides, f_p decreased significantly in the normal group (36.28 ± 9.70 (%) vs. 29.93 ± 10.25 (%), $p = 0.032$) post hyperoxygenation, whereas it kept relatively stable in the FGR group (22.88 ± 10.29 (%) vs. 24.38 ± 13.67 (%), $p = 0.508$). For D_t, the values in normal group increased significantly (1.47 ± 0.23 $(10^{-3})mm^2/sec$ vs. 1.86 ± 0.42 $(10^{-3})mm^2/sec$, $p = 0.000$), but no significant changes were found for the FGR group (1.22 ± 0.29 $(10^{-3})mm^2/sec$ vs. 1.17 ± 0.19 $(10^{-3})mm^2/sec$, $p = 0.508$). For D_p, no significant changes were found for both normal (63.42 ± 54.18 $(10^{-3})mm^2/sec$ vs. 63.08 ± 35.89 $(10^{-3})mm^2/sec$, $p = 0.43$) and FGR (51.82 ± 53.28 $(10^{-3})mm^2/sec$ vs. 83.04 ± 63.83 $(10^{-3})mm^2/sec$, $p = 0.13$) groups.

Furthermore, Fig. 4 provided the plot of f_p for each subject in both groups and their relative percentage change, Δf, after maternal hyperoxygenation. The mean changes and median changes of Δf due to hyperoxygenation were −12.2% and −10.1% as well as 7.9% and 15.3% for the normal and FGR groups, respectively. However, there were not statistical difference between two groups ($p = 0.154$).

3.4. The correlation between Doppler findings and IVIM derived parameter

Furthermore, the correlation between Doppler findings—umbilical artery pulsatility index (PI) and IVIM parameters was also quantified via Spearman correlative coefficients abbreviated as r. As Fig. 5 displayed, no significant correlations were found in normal patients group and FGR patients group. Interestingly, there existed negative correlation between PI and IVIM-derived parameters including $f_{p\,pre}$ ($r = -0.385$, $p < 0.05$) and $D_{t\,post}$ ($r = -0.574$, $p < 0.01$) for all patients group (n = 35).

3.5. Diagnostic value of IVIM-derived parameter for discriminating the FGR patients from normal patients

Moreover, the diagnostic value of IVIM-derived parameter was also evaluated via ROC analysis (Fig. 6). Among three parameter including $f_{p\,pre}$, $D_{t\,pre}$ and $D_{t\,post}$, showing significant statistical difference between normal patients and FGR patients, $f_{p\,pre}$ displayed a best diagnostic

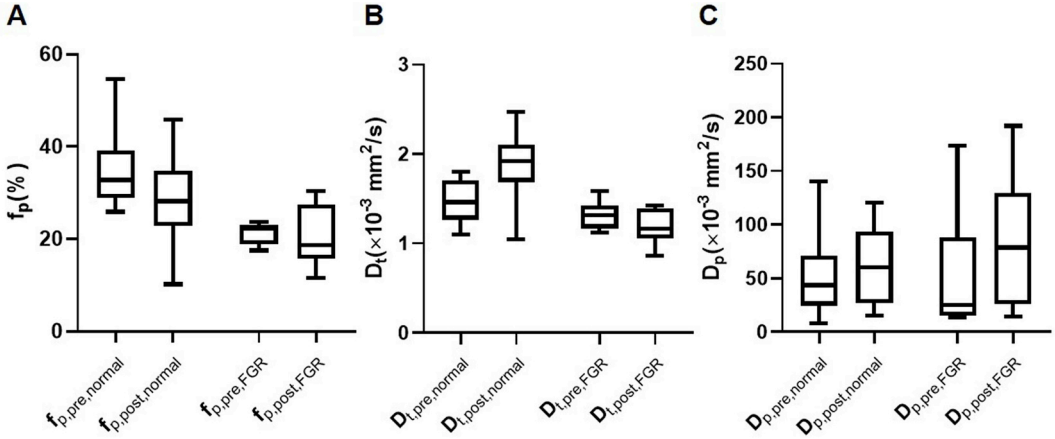

Fig. 3. Box plot of IVIM parameters for normal and FGR groups before and after oxygenation inhalation: A: perfusion fraction (f_p); B: true diffusivity (D_t); C: Pseudo diffusivity (D_p). The top and bottom of each box represent the 25% and 75% percentiles, respectively, for all parameters. The horizontal line inside each box represents the median value.

Table 4
Comparative analysis of all IVIM parameters within and between normal and FGR groups.

Comparison			P value
Within groups:			
$f_{p,pre,normal}$	versus	$f_{p,post,normal}$	0.032
$D_{t,pre,normal}$	versus	$D_{t,post,normal}$	0.000
$D_{p,pre,normal}$	versus	$D_{p,post,normal}$	0.427
$f_{p,pre,FGR}$	versus	$f_{p,post,FGR}$	0.508
$D_{t,pre,FGR}$	versus	$D_{t,post,FGR}$	0.508
$D_{p,pre,FGR}$	versus	$D_{p,post,FGR}$	0.114
Between groups:			
$f_{p,pre,normal}$	versus	$f_{p,pre,FGR}$	0.000
$D_{t,pre,normal}$	versus	$D_{t,pre,FGR}$	0.037
$D_{p,pre,normal}$	versus	$D_{p,pre,FGR}$	0.307
$f_{p,post,normal}$	versus	$f_{p,post,FGR}$	0.058
$D_{t,post,normal}$	versus	$D_{t,post,FGR}$	0.000
$D_{p,post,normal}$	versus	$D_{p,post,FGR}$	0.577

Note.-* FGR – Fetal growth restricted; IVIM – Intravoxel incoherement motion; f_p – perfusion fraction; D_t – true diffusivity; D_p – pseudodiffusivity.

value with the area under curve (AUC) of 0.912 in comparison to $D_{t\ pre}$ with AUC of 0.728 and $D_{t\ post}$ with AUC of 0.904. The other diagnostic indexes sourced from ROC curve were displayed in Table 5.

4. Discussion

Evolving from traditional mono-exponential DWI, IVIM was firstly proposed in 1980s. The most significant hypothesis of IVIM lies in that the distribution of water Brownian motion in each voxel is based on two-components model. The first component is mainly applied for explaining the microscopic intravascular motion of water molecule flowing in the capillary network. The characteristic parameters in this component contains the f_p (perfusion fraction) and D_p (pseudo diffusion coefficients). Relative high value of f_p signifies the hyper-vascularity and hyper-perfusion. For instance, it was reported that the low f_p is an effective early diagnostic indicator of hypo-perfusion in placenta [14]. As for D_p, the increased value indicates the increased capillary flow velocity microscopically manifested as less impediment of water Brownian motion in capillary. Differently, the other one – extravascular component represents the water Brownian motion between cells. The characteristic parameter, D_t (True Diffusion Coefficients), can offer the insight of cellularity: the decreased value of D_t implies the more restricted extra-cellular diffusion space caused by increased cellularity. For example, the decreased D_t plays significant role in indicating the malignant carcinogenesis in oncology [16].

In this study, $f_{p,pre}$ was found to be significantly lower in the FGR group than that in normal group together with the results that both $D_{t\ pre}$ and $D_{t\ post}$ is lower in FGR group than that of normal patients group. These results could be explained by the following points:

1) The increased vascular resistance as well as the peripheral hypovascularity leaded to the far limited microcirculation for FGR patients, represented as the distinguishable decrease of f_p [4–6].
2) Placental abnormalities of FGR noted above, potentially leading to the hyper-cellularity, is closely associated with the more restricted diffusion representing as the decreased Diffusion coefficients (IVIM derived D_t or traditional DWI derived apparent Diffusion Coefficients(ADC)) [14,17].

After hyper-oxygenation, the significant decrease of f_p as well as increase of D_t could be explained by the following reasons:

1) An increase of cellular interstitial space caused by hyperoxygenation, prudently speculated by us, may resulted in a far less restricted diffusion space appearing as the increased D_t. However, the mechanics of how the placenta environment changes during hyperoxygenation reflected by the both f_p and D_t needs further investigation because there were scarce evidence and limited related research.
2) Several previous studies provided the evidence of that Hyperoxygenation will result in the obviously decreased synthesis of prostacyclin—vasodilator, leading to the reduced perfusion. Additionally, high O_2 content would also cause the direct vasoconstrictor effect [18–20]. Therefore, the significant decrease of f_p occurred as the result of the maternal hyperoxygenation.

It was also worthwhile to be noted that there existed some reasons causing the fact that no significant statistical difference between normal and FGR patients pre and post the maternal oxygenation.

1) Relative small sample size definitely resulted in some unexpected influence. For instance, critical p value of 0.058 was obtained while the $f_{p,post,normal}$ and $f_{p,post,FGR}$ was compared. 2) Always vulnerable to the low Signal to Noise Ratio (SNR), D_p is always incapable of offering a statistical conclusion with significance [21,22]. 3) No significant changes of f_p were found for FGR group after maternal hyperoxygenation. This low sensitivity of f_p to maternal hyperoxygenation might be attributed to the lower baseline of placental perfusion due to placental insufficiency in the FGR group.

In addition, our results offered the results that Doppler findings—PI negatively correlated with the IVIM derived parameter, in accordance with the previous investigation [23]. Several explanations were listed as the followings:

1) As gestational ages increases, inadequate maternal vascular response to placentation leads to increased impedance to flow

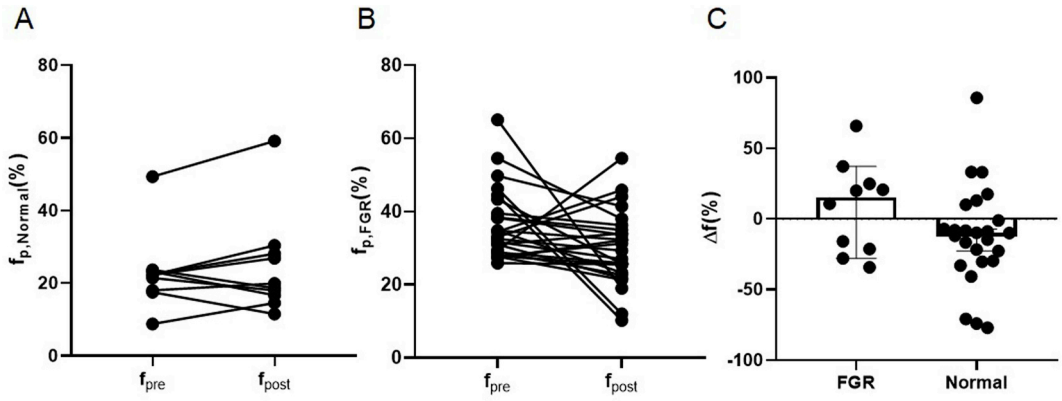

Fig. 4. Perfusion fraction (f_p) and relative percentage changes (Δf) for each subject were presented. f_p for each subject in FGR group (A) and normal group (B) pre and post maternal hyperoxygenation; C: relative percentage changes (Δf) for each patient in FGR group and normal group.

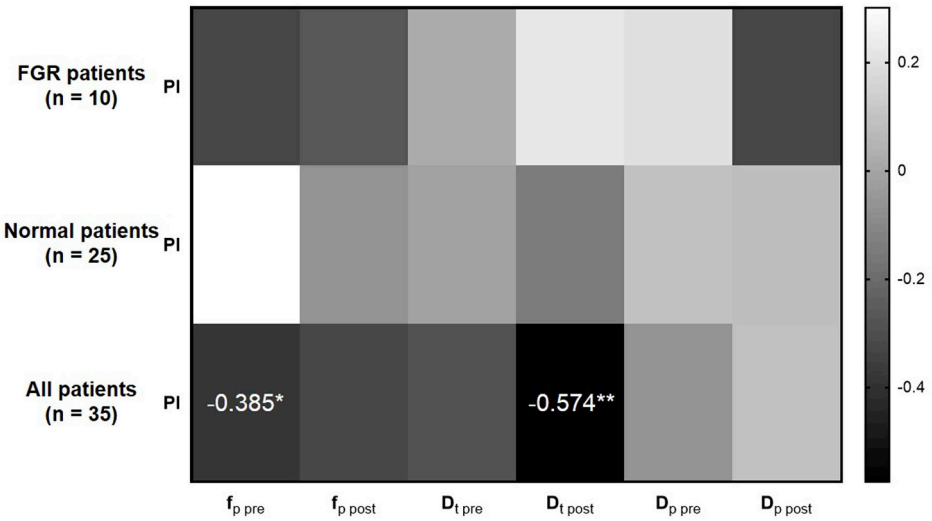

Fig. 5. Heat map, depicting the Spearman correlation between IVIM parameters and Doppler findings (*: $p < 0.05$, **: $p < 0.01$).

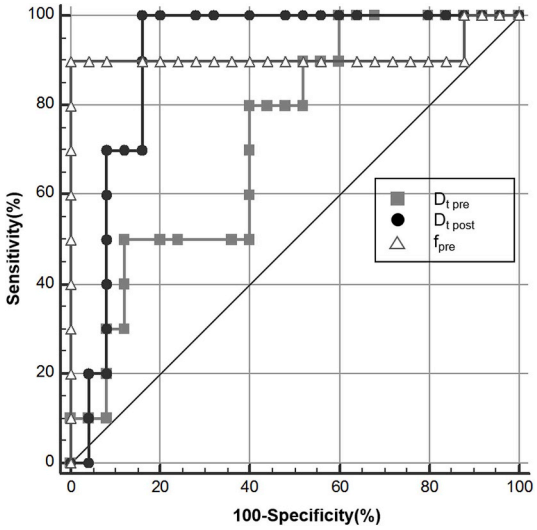

Fig. 6. ROC analysis for discriminating FGR patients from normal counterparts with IVIM derived parameters including $D_{t\ pre}$, $D_{t\ post}$ and $f_{p\ pre}$.

Table 5
ROC curve derived parameter for determining the diagnostic power of parameter sourced from IVIM.

Parameter	Sensitivity (%)	Specificity (%)	AUC	Youden Index
$f_{p\ pre}$	90.000	100.000	0.912	0.900
$D_{t\ pre}$	80.000	60.000	0.728	0.400
$D_{t\ post}$	100.000	84.000	0.904	0.840

measured by the uterine artery PI on Doppler ultrasound [23].

2) It was reported that, up to 25 weeks of pregnancy, some non-branching vessels appears to be vascularized and matured on the fetal side [24]. From that time point, the placental angiogenesis was outpaced by placenta growth [25], resulting in a relative decline in the placenta perfusion fraction (f).
3) Jakab's findings suggests that D_t decreases as gestational age increases [26]. Besides, owning similar biological implication, ADC (Apparent Diffusion Coefficient) decreases as the function of gestational weeks in the previous research [14]. These results indicates that extracellular space in placenta become more restricted due to the placental growth.

In general, as aforementioned points, D_t and f_p decreased but PI increased as the function of gestational week. It's understandable that D_t and f_p negatively correlated with PI. Vulnerable to the influence of low SNR, D_p always displayed no statistical difference compared to D_t and f_p. It's worthwhile to be noted that the correlation with statistical difference between IVIM results and Doppler findings only existed in the all patients group (n = 35) but no statistical correlation was found in FGR patients group (n = 10) and normal patients group (n = 25). The relative small sample size, prudently speculated by us, was the leading cause, implying that enlarged sample size especially the number of FGR patients will be recommendable in the subsequent research.

Moreover, the ROC analysis result: $f_{p\ pre}$ had the best diagnostic value of all IVIM-derived parameter for discriminating FGR patients from normal patients indicated that compared to other biological indexes, the perfusion variation is one essential biological implication holding great potential for diagnosing FGR patients. On the other hand, above results also implied that IVIM had great clinical value for evaluating the perfusion of FGR patients.

Several limitations should be acknowledged in this study. First, the finding obtained in this study was preliminary and based on a limited number of FGR pregnancies; a further large cohort of FGR cases or multi-center study are necessary. Second, two IVIM examinations were performed in this study, which may introduce additional error for ROI analysis for potential spatial mis-registration, although we delineated the ROI in the central part of placenta which might be less susceptible to such spatial error. Correcting for motion correction is another concern to keep data from more patients.

In conclusion, this research provided the insight that the significant difference not merely existed in the placental perfusion level but also existed in the response of maternal hyperoxygenation for both normal patients and FGR patients with aid of IVIM. Furthermore, IVIM derived parameter displayed high diagnostic power for discriminating FGR patients from normal counterparts, implying IVIM had great clinic value for evaluating the perfusion of FGR patients.

Financial support

This study was supported by grants from the Maternal and Child Health research project of Jiangsu province, China [grant number No.F201845].

Conflicts of interest

The authors declare that they have no conflict of interest.

References

[1] F. Figueras, E. Gratacos, Update on the diagnosis and classification of fetal growth restriction and proposal of a stage-based management protocol, Fetal Diagn. Ther. 36 (2) (2014) 86–98.

[2] M. Alberry, P. Soothill, Management of fetal growth restriction, Arch. Dis. Child Fetal. Neonatal. Ed. 92 (1) (2007) F62–F67.

[3] T.A. Levine, R.E. Grunau, F.M. McAuliffe, R. Pinnamaneni, A. Foran, F.A. Alderdice, Early childhood neurodevelopment after intrauterine growth restriction: a systematic review, Pediatrics 135 (1) (2015) 126–141.

[4] J.S. Cnossen, R.K. Morris, G. ter Riet, B.W. Mol, J.A. van der Post, A. Coomarasamy, A.H. Zwinderman, S.C. Robson, P.J. Bindels, J. Kleijnen, K.S. Khan, Use of uterine artery Doppler ultrasonography to predict pre-eclampsia and intrauterine growth restriction: a systematic review and bivariable meta-analysis, CMAJ : Can. Med. Assoc. J. = journal de l'Association medicale canadienne 178 (6) (2008) 701–711.

[5] E. Ingram, D. Morris, J. Naish, J. Myers, E. Johnstone, MR imaging measurements of altered placental oxygenation in pregnancies complicated by fetal growth restriction, Radiology 285 (3) (2017) 953–960.

[6] T.O. Junaid, P. Brownbill, N. Chalmers, E.D. Johnstone, J.D. Aplin, Fetoplacental vascular alterations associated with fetal growth restriction, Placenta 35 (10) (2014) 808–815.

[7] T. Perreault, F. Coceani, Endothelin in the perinatal circulation, Can. J. Physiol. Pharmacol. 81 (6) (2003) 644–653.

[8] I. Rodriguez, M. Gonzalez, Physiological mechanisms of vascular response induced by shear stress and effect of exercise in systemic and placental circulation, Front. Pharmacol. 5 (2014) 209.

[9] L. Myatt, Review: reactive oxygen and nitrogen species and functional adaptation of the placenta, Placenta 31 (Suppl) (2010) S66–S69.

[10] K.H. Nicolaides, S. Campbell, R.J. Bradley, C.M. Bilardo, P.W. Soothill, D. Gibb, Maternal oxygen therapy for intrauterine growth retardation, Lancet 1 (8539) (1987) 942–945.

[11] L. Say, A.M. Gulmezoglu, G.J. Hofmeyr, Maternal oxygen administration for suspected impaired fetal growth, Cochrane Database Syst. Rev. (1) (2003) Cd000137.

[12] L. Tang, X.J. Zhou, Diffusion MRI of cancer: from low to high b-values, J. Magn. Reson. Imaging : JMRI 49 (1) (2019) 23–40.

[13] C. Federau, Intravoxel incoherent motion MRI as a means to measure in vivo perfusion: a review of the evidence, NMR Biomed. 30 (11) (2017).

[14] N. Siauve, P.H. Hayot, B. Deloison, G.E. Chalouhi, M. Alison, D. Balvay, L. Bussieres, O. Clement, L.J. Salomon, Assessment of human placental perfusion by intravoxel incoherent motion MR imaging, J. Matern. Fetal Neonatal Med. : Off. j. Eur. Assoc. Perinat. Med. Fed. Asia Oceania Perinat. Soc. Int. Soc. Perinat. Obstet. 32 (2) (2019) 293–300.

[15] T. Callahan, A.B. Caughey, Blueprints Obstetrics and Gynecology, Lippincott Williams & Wilkins, 2013.

[16] S. Woo, J.M. Lee, J.H. Yoon, I. Joo, J.K. Han, B.I. Choi, Intravoxel incoherent motion diffusion-weighted MR imaging of hepatocellular carcinoma: correlation with enhancement degree and histologic grade, Radiology 270 (3) (2014) 758–767.

[17] H.M. Bonel, B. Stolz, L. Diedrichsen, K. Frei, B. Saar, B. Tutschek, L. Raio, D. Surbek, S. Srivastav, M. Nelle, J. Slotboom, R. Wiest, Diffusion-weighted MR imaging of the placenta in fetuses with placental insufficiency, Radiology 257 (3) (2010) 810–819.

[18] D.C. Kuhn, M.J. Stuart, Cyclooxygenase inhibition reduces placental transfer: reversal by carbacyclin, Am. J. Obstet. Gynecol. 157 (1) (1987) 194–198.

[19] B.N. Yamaja Setty, R.W. Walenga, M.J. Stuart, Kinetic analyses of the effects of hyperoxia and hypoxia on vascular cyclooxygenase activity in vitro, Biochem. Biophys. Res. Commun. 125 (1) (1984) 170–176.

[20] D.C. Kuhn, M.A. Crawford, G.B. Gordon, M.J. Stuart, Aspects of in vitro placental perfusion: effects of hyperoxia and phenol red, Placenta 9 (2) (1988) 201–213.

[21] M. Klauss, P. Mayer, K. Maier-Hein, F.B. Laun, A. Mehrabi, H.U. Kauczor, B. Stieltjes, IVIM-diffusion-MRI for the differentiation of solid benign and malign hypervascular liver lesions-Evaluation with two different MR scanners, Eur. J. Radiol. 85 (7) (2016) 1289–1294.

[22] Y. Wei, F. Gao, M. Wang, Z. Huang, H. Tang, J. Li, Y. Wang, T. Zhang, X. Wei, D. Zheng, B. Song, Intravoxel incoherent motion diffusion-weighted imaging for assessment of histologic grade of hepatocellular carcinoma: comparison of three methods for positioning region of interest, Eur. Radiol. 29 (2) (2019) 535–544.

[23] I. Derwig, D.J. Lythgoe, G.J. Barker, L. Poon, P. Gowland, R. Yeung, F. Zelaya, K. Nicolaides, Association of placental perfusion, as assessed by magnetic resonance imaging and uterine artery Doppler ultrasound, and its relationship to pregnancy outcome, Placenta 34 (10) (2013) 885–891.

[24] F. Herr, N. Baal, R. Widmer-Teske, T. McKinnon, M. Zygmunt, How to study placental vascular development? Theriogenology 73 (6) (2010) 817–827.

[25] M. Zygmunt, F. Herr, K. Munstedt, U. Lang, O.D. Liang, Angiogenesis and vasculogenesis in pregnancy, Eur. J. Obstet. Gynecol. Reprod. Biol. 110 (Suppl 1) (2003) S10–S18.

[26] A. Jakab, R.L. Tuura, R. Kottke, N. Ochsenbein-Kolble, G. Natalucci, T.D. Nguyen, C. Kellenberger, I. Scheer, Microvascular perfusion of the placenta, developing fetal liver, and lungs assessed with intravoxel incoherent motion imaging, J. Magn. Reson. Imaging : JMRI 48 (1) (2018) 214–225.